Molecular Simulation Study of Swelling Clays

Arun Kumar Narayanan Nair

May, 2018

King Abdullah University of Science & Technology (KAUST),
Physical Science and Engineering Division,
Computational Transport Phenomena Laboratory,
Thuwal, 23955-6900, Saudi Arabia.

Shale

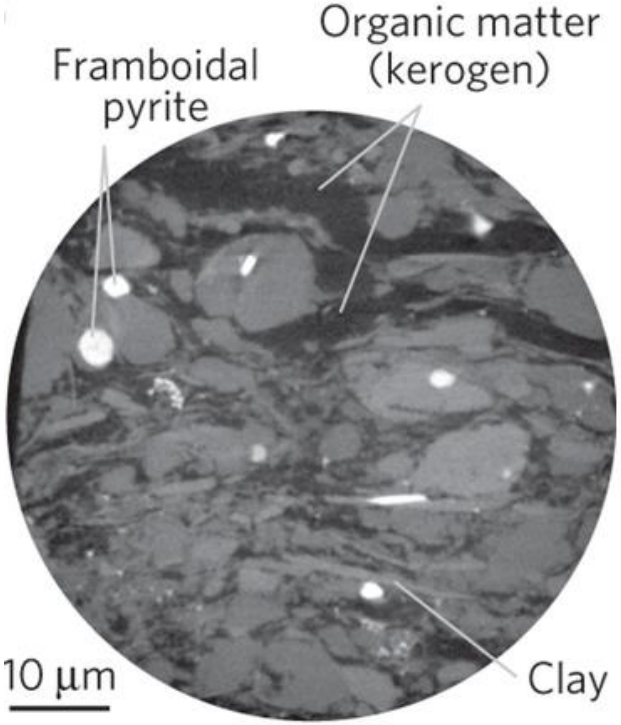

Bousige et al., 2016

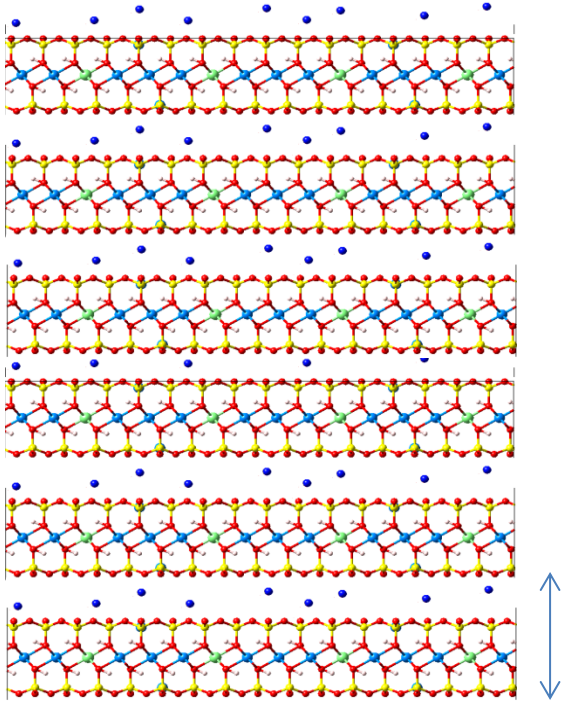

basal spacing, d

Clay

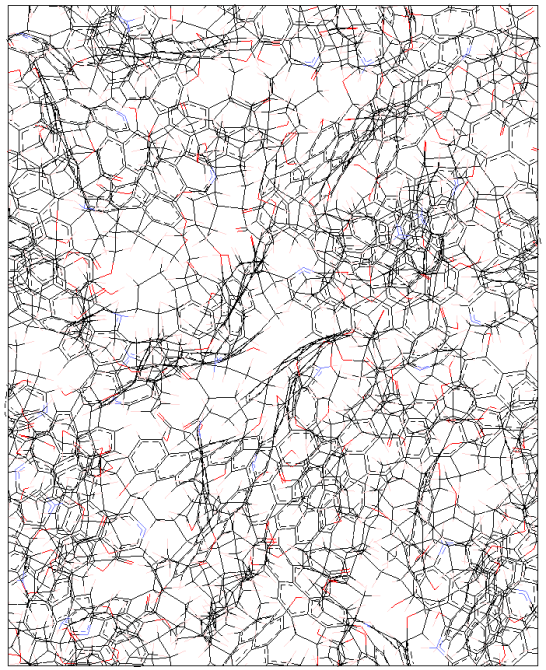

Kerogen

Simulation methods

Our focus:

• Grand Canonical Monte Carlo (GCMC) simulations: adsorption amount of gases (μVT ensemble), where μ is the chemical potential, V is the volume and T is the temperature.

• Molecular dynamics (MD) simulations: diffusion coefficients of gases (NVT ensemble), where N is the number of particles.

Monte Carlo simulations

• Probability P_i of the system to be found in a state i with energy E_i is proportional to its statistical weight. For example, in an NVT ensemble

$$P_i \sim \exp\left(-\frac{E_i}{kT}\right)$$

• Detailed balance: the probability of being in the state i and transit to the state j is equal to the probability of being in the state j and transit to the state i.

$$P_i g_{i\to j} p_{i\to j} = P_j g_{j\to i} p_{j\to i}$$

$g_{i\to j}p_{i\to j}$ - transition probability

$g_{i\to j}$ - probability of making an attempt to move from state i to state j

$p_{i\to j}$ - probability of accepting attempted transition

Metropolis algorithm

- Probability of making an attempt to move

$$g_{j\to i} = g_{i\to j}$$

- Probability of accepting attempted transition

$$p_{i\to j} = 1 \quad \text{if } E_j \le E_i$$

$$p_{i\to j} = \exp\left(-\frac{E_j - E_i}{kT}\right) \quad \text{if } E_j > E_i$$

- Grand canonical ensemble (addition or deletion of particles)

$$P_{\text{acc}}^{N\to N+1} = \min\left[1, \quad \frac{V}{\Lambda^3(N+1)}\exp[\beta(\mu - \Delta E)]\right]$$

$$P_{\text{acc}}^{N+1\to N} = \min\left[1, \quad \frac{\Lambda^3(N)}{V}\exp[-\beta(\mu + \Delta E)]\right]$$

de Broglie thermal wavelength $\lambda = h/\sqrt{2\pi mkT}$

Molecular dynamics simulations

- Numerical integration of Newton's equations of motion for a system of particles.
- N-particle system with potential energy

$$U(\vec{r}_1, \vec{r}_2, \cdots \vec{r}_N) = U(\vec{R})$$

- 3N coupled 2nd-order differential equations.

$$m_i \frac{d^2 \vec{r}_i}{dt^2} = \vec{F}_i = -\vec{\nabla} U(\vec{R}) \quad = -\left(\frac{\partial U}{\partial x_i}, \frac{\partial U}{\partial y_i}, \frac{\partial U}{\partial z_i} \right)$$

$$i \quad = 1, \ldots, N$$

- Propagated forward (or backward) in time.
- Initial coordinates obtained from, e.g., crystal structure, velocities taken at random from Boltzmann distribution.
- Maintain appropriate temperature by adjusting velocities.

Intermolecular model potential

Lennard-Jones 12–6 potential

$$v^{\mathrm{LJ}}(r) = 4\varepsilon\left[\left(\frac{\sigma}{r}\right)^{12} - \left(\frac{\sigma}{r}\right)^{6}\right]$$

ϵ governs the strength of the interaction

σ defines a length scale

$$r = |\boldsymbol{r}_i - \boldsymbol{r}_j|$$

long-range attractive tail of the form $-1/r^6$

steeply rising repulsive wall at distances less than $r \sim \sigma$.

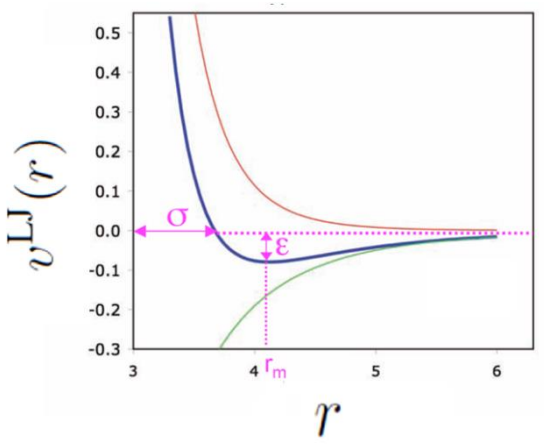

Attractive:
induced dipole / induced dipole

$$\propto -\frac{1}{r^6}$$

Repulsive :
Pauli exclusion principle

$$\propto \frac{1}{r^{12}}$$

liquid argon

$\varepsilon/k_B \approx 120$ K and $\sigma \approx 0.34$ nm

r_m : distance at min $\quad r_m = 2^{1/6}\sigma$

Intermolecular model potential

Coulomb energy E $= \frac{1}{4\pi\varepsilon_0}\sum_{i<j}\frac{q_i q_j}{|\mathbf{r_i}-\mathbf{r_j}|} = \frac{1}{8\pi\varepsilon_0}\sum_{i\neq j}\frac{q_i q_j}{|\mathbf{r_i}-\mathbf{r_j}|}.$

$$E = \frac{1}{2}\sum_{i,j=1}^{N}{}' \sum_{\boldsymbol{n}\in\mathbb{Z}^3}\frac{q_i q_j}{|\boldsymbol{r}_{ij}+\boldsymbol{n}L|}$$

$$\boldsymbol{n} = (n1, n2, n3) = n_1\boldsymbol{L}\boldsymbol{x} + n_2\boldsymbol{L}\boldsymbol{y} + n_3\boldsymbol{L}\boldsymbol{z}$$

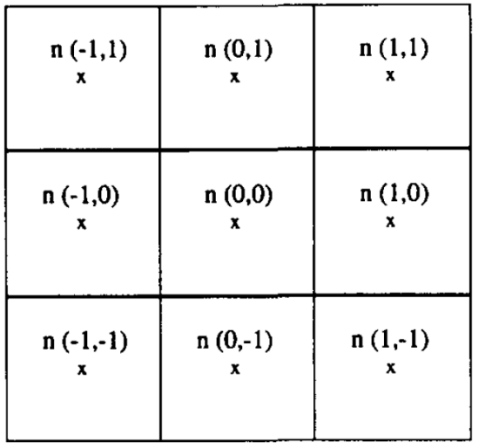

- Interatomic potentials derived from parametrizations incorporating structural (X-ray) and spectroscopic data (NMR)
- Partial charges derived by Mulliken and electrostatic potential (ESP) analysis of DFT results

Cygan, et al., 2004

CLAYFF Force Field

species	symbol	charge (e)	D_o (kcal/mol)	R_o (Å)
water hydrogen	h*	0.4100		
hydroxyl hydrogen	ho	0.4250		
water oxygen	o*	−0.8200	0.1554	3.5532
hydroxyl oxygen	oh	−0.9500	0.1554	3.5532
bridging oxygen	ob	−1.0500	0.1554	3.5532
bridging oxygen with octahedral substitution	obos	−1.1808	0.1554	3.5532
bridging oxygen with tetrahedral substitution	obts	−1.1688	0.1554	3.5532
bridging oxygen with double substitution	obss	−1.2996	0.1554	3.5532
hydroxyl oxygen with substitution	ohs	−1.0808	0.1554	3.5532
tetrahedral silicon	st	2.1000	1.8405×10^{-6}	3.7064
octahedral aluminum	ao	1.5750	1.3298×10^{-6}	4.7943
tetrahedral aluminum	at	1.5750	1.8405×10^{-6}	3.7064
octahedral magnesium	mgo	1.3600	9.0298×10^{-7}	5.9090
hydroxide magnesium	mgh	1.0500	9.0298×10^{-7}	5.9090
octahedral calcium	cao	1.3600	5.0298×10^{-6}	6.2484
hydroxide calcium	cah	1.0500	5.0298×10^{-6}	6.2428
octahedral iron	feo	1.5750	9.0298×10^{-6}	5.5070
octahedral lithium	lio	0.5250	9.0298×10^{-6}	4.7257
aqueous sodium ion[a]	Na	1.0	0.1301	2.6378
aqueous potassium ion[b]	K	1.0	0.1000	3.7423
aqueous cesium ion[c]	Cs	1.0	0.1000	4.3002
aqueous calcium ion[b]	Ca	2.0	0.1000	3.2237
aqueous barium ion[d]	Ba	2.0	0.0470	4.2840
aqueous chloride ion[a]	Cl	−1.0	0.1001	4.9388

$$E_{\mathrm{VDW}} = \sum_{i\neq j} D_{\mathrm{o},ij}\left[\left(\frac{R_{\mathrm{o},ij}}{r_{ij}}\right)^{12} - 2\left(\frac{R_{\mathrm{o},ij}}{r_{ij}}\right)^{6}\right]$$

Intramolecular interaction

$$U(\vec{R}) = \sum_{\text{bonds}} K_b(b - b_0)^2 + \sum_{\text{angle}} K_\theta(\theta - \theta_0)^2 + \sum_{\textit{dihedrals}} u_{\text{dih}}(\phi) + \cdots$$

The harmonic potential is a Taylor approximation of more elaborate potentials around the reference bond length

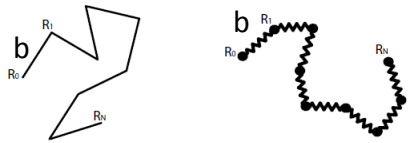

b= bond length

b_0=equilibrium bond length

κ_b = spring constant

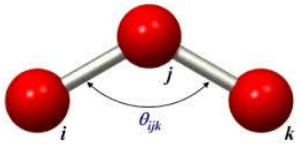

θ= bond angle

θ_0= equilibrium bond angle

k_θ =bending constant

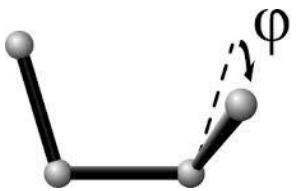

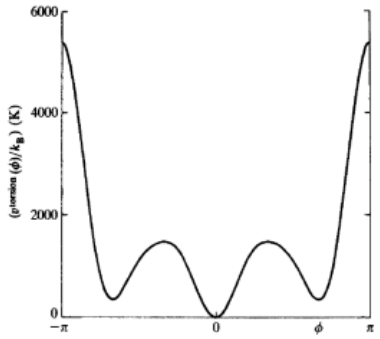

- Usually a cosine series for dihedral interactions.

General classes of clays

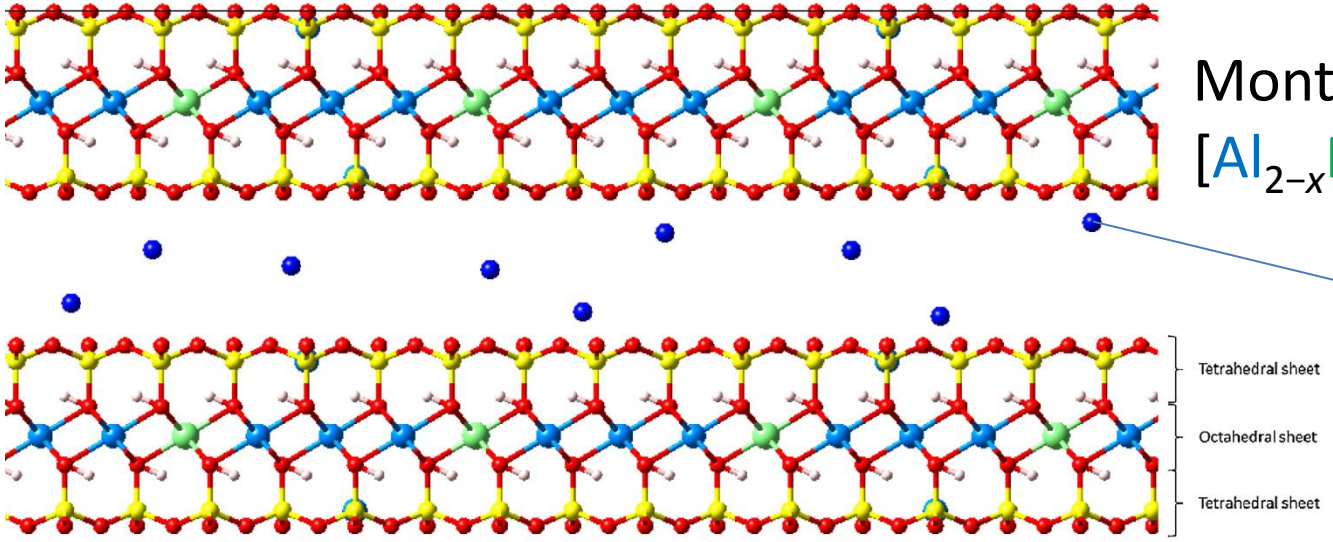

Montmorillonite:

$[Al_{2-x}Mg_x][Si_{4-z}Al_z]O_{10}(OH)_2$

counterions:

Na^+, K^+, Ca^{2+}

• For tri- (3 divalent cations in the octahedral site) and di-octahedral (2 trivalent cations in the octahedral site) structural formulae, $[T_{3-x}M_x][Si_{4-z}Al_z]O_{10}(OH)_2$ and $[D_{2-x}M_x][Si_{4-z}Al_z]O_{10}(OH)_2$, then based on the total layer charge, $Q = x + z$:

- Talcs and pyrophyllite: $Q \sim 0.0$. **Non-swelling** hydrophobic clays.

- Smectites: $0.2 < Q < 0.6$. **Swelling clays**, individual platelet size $\sim\mu m^2$.

- Vermiculites: $0.6 < Q < 0.9$. **Swelling clays**, individual platelet sizes $\sim mm^2$.

- Illites and micas: $0.9 < Q < 1.0$. **Non-swelling** hydrophilic clays.

Skipper et al., 2006

Water uptake by swelling clays (Na-montmorillonite)

- Quantitative agreement of simulated water content in clays with experimental data.
- Water shows layered structures.

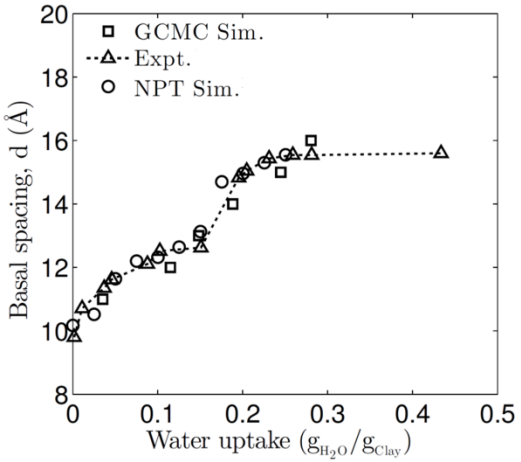

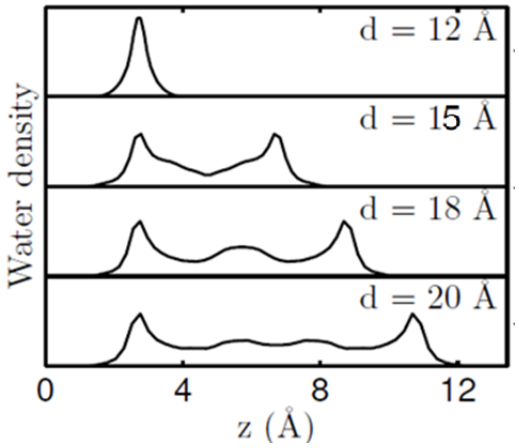

d=12 Å

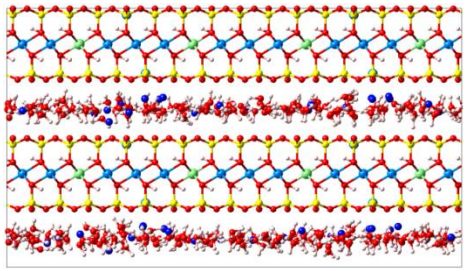

d=15 Å

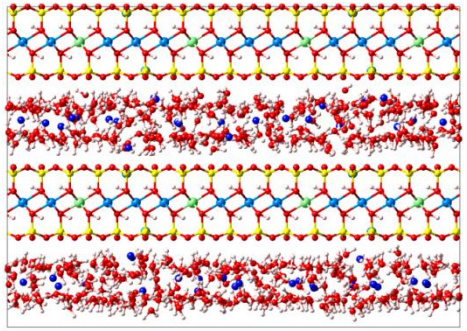

d=18 Å

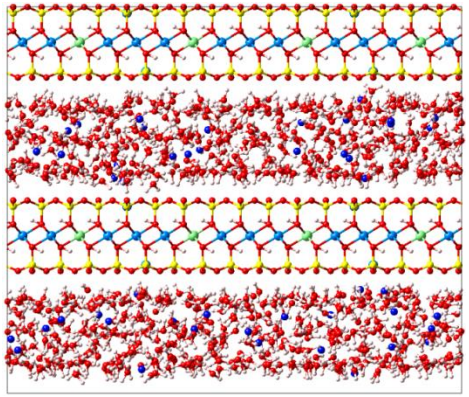

H_2O

Na^+

Kadoura et al., 2016a

Diffusion of water and ions in montmorillonite

- MD simulation study (NVT) at 298 K
- Mean square displacement (MSD) versus time

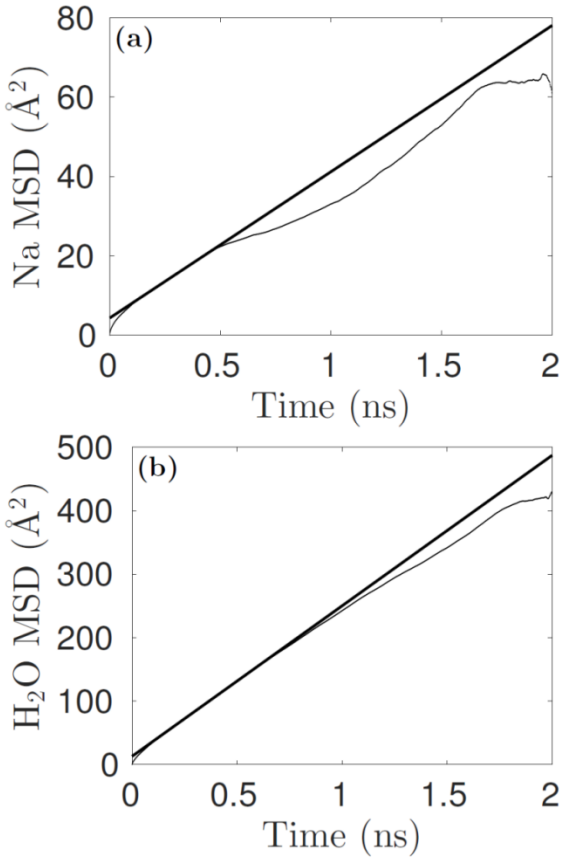

Einstein relation

$$D_{\mathrm{xy}} = \lim_{t\to\infty} \frac{1}{4N_m t} \left\langle \sum_{j=1}^{N_m} [r_j(t) - r_j(0)]^2 \right\rangle$$

Diffusion of water and ions in Na-montmorillonite

• Quantitative agreement of simulated self-diffusion coefficients of water and ions in clays with experimental data.

• Decrease by about 1–3 orders of magnitude under the extreme confinement compared to bulk.

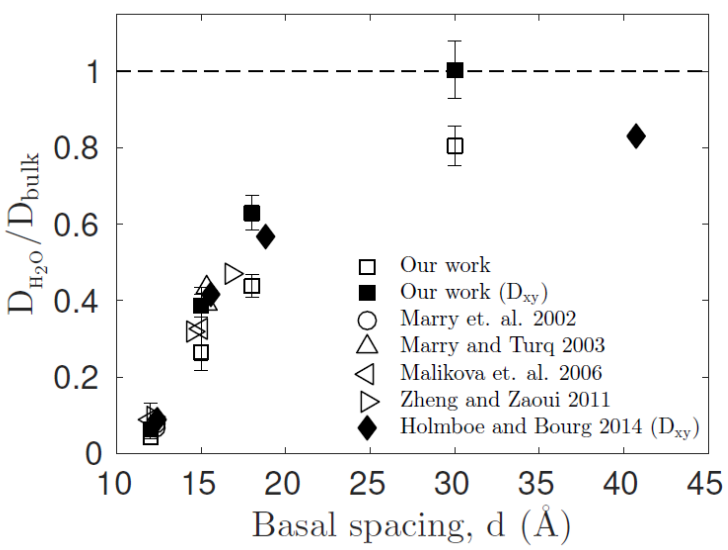

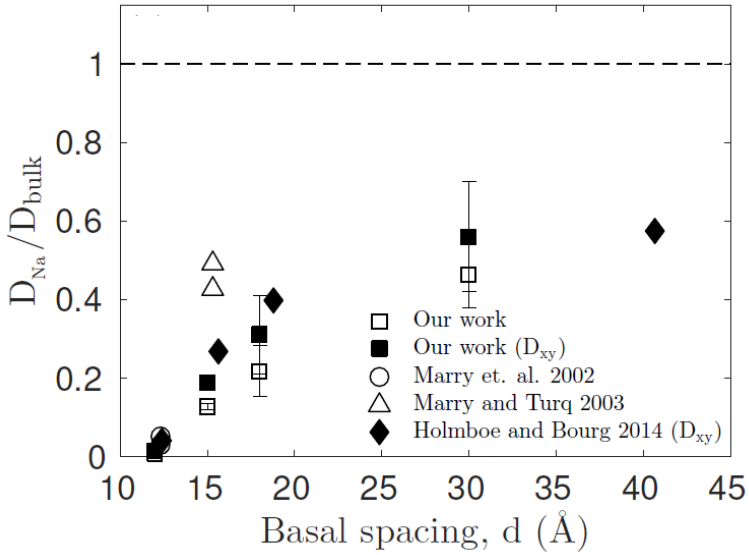

Kadoura et al., 2016b

Adsorption of CO2 and CH4 by montmorillonite in the presence of water

• GCMC simulation study in the presence of pre-adsorbed water (μ_{CO2}VT or μ_{CH4}VT)

• Atomistic model gives reasonable agreement with single-component experimental adsorption isotherms for CH4 and CO2 molecules

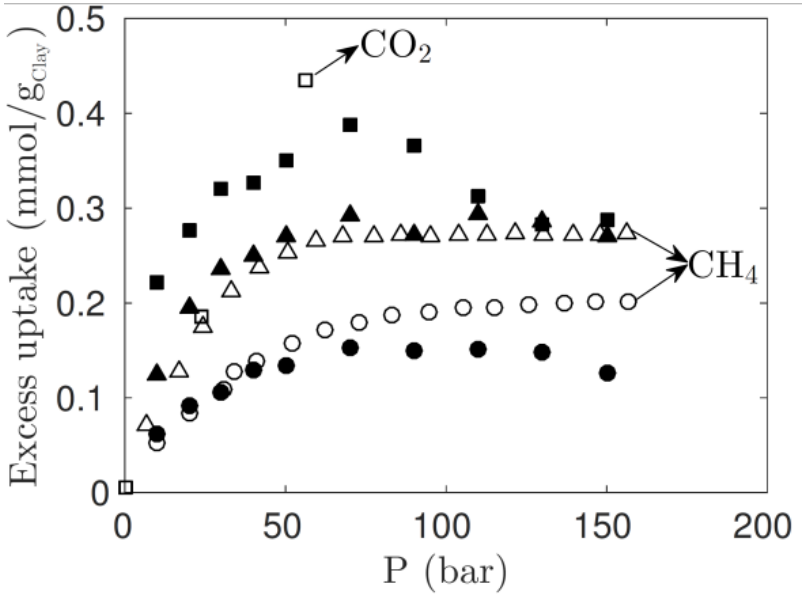

• Expt. at about 60 °C (open symbols)
• GCMC simulations (solid symbols)
• Water contents: 0.4 (squares), 0.5 (triangles), and 0.55 g/cm^3 (circles)
• d=12 Å (CO2)
• d=15 Å (CH4)

Kadoura et al., 2016a

Adsorption of CO2 and CH4 by montmorillonite in the presence of water

• Favorability of adsorption of CO2 (and CH4 to a lesser extent) by montmorillonite at intermediate water contents.

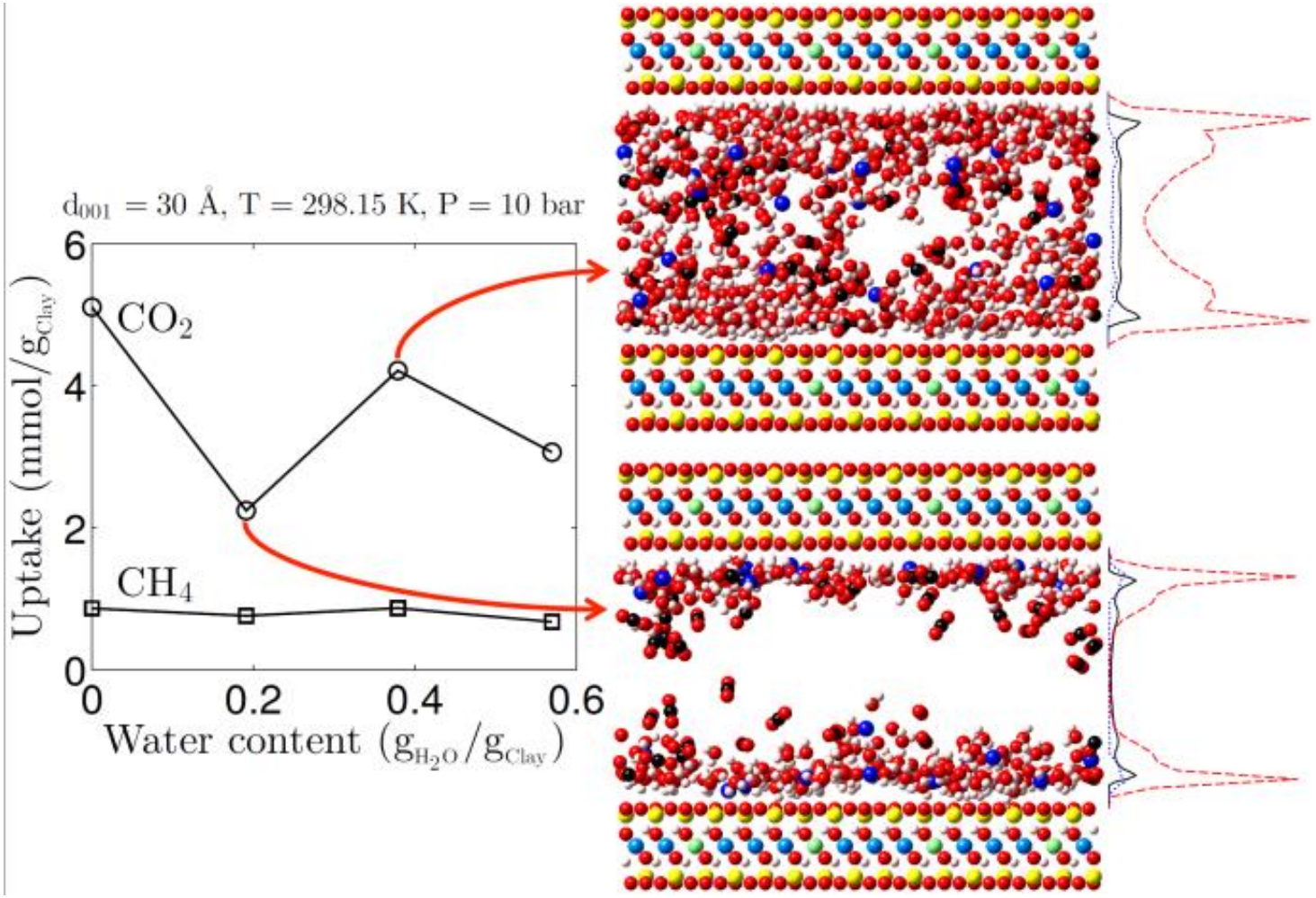

Adsorption of CO2 and CH4 by montmorillonite in the presence of water

- Favorability of adsorption of CO2 (and CH4 to a lesser extent) by montmorillonite at small basal spacing d.

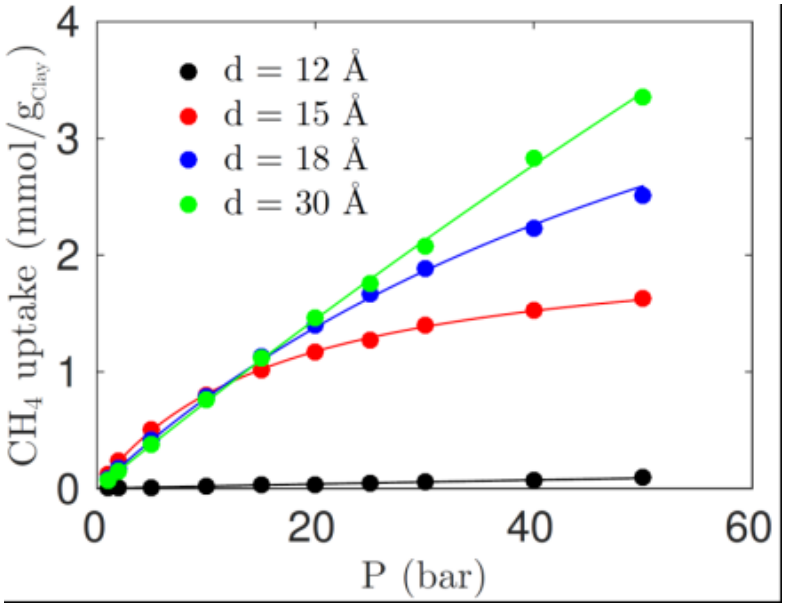

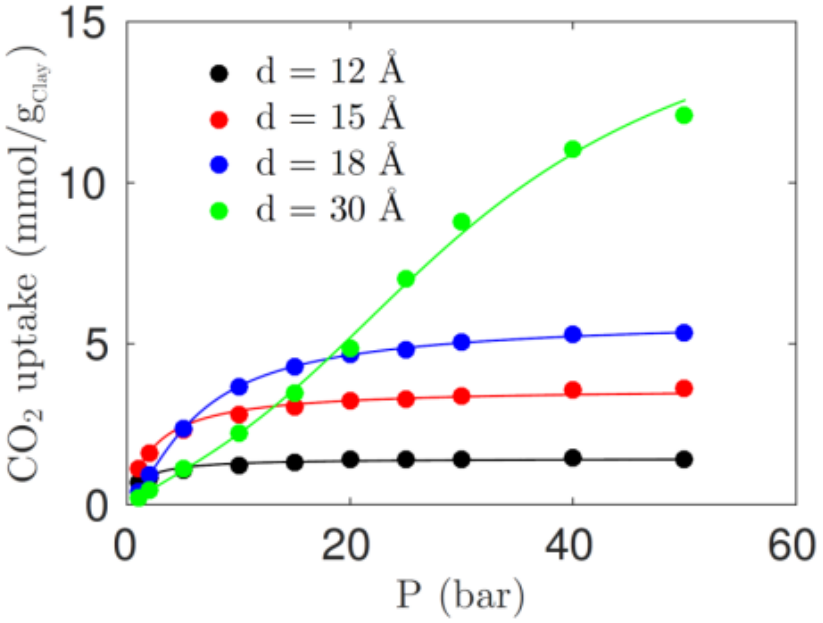

- Water content: 0.2 g/cm^3
- T=298 K

Adsorption of CO2/CH4 mixture by montmorillonite in the presence of water

• GCMC simulation study of adsorption of CO2/CH4 mixture in montmorillonite clays in the presence of water (pre-adsorbed) at 298 K ($\mu_{CO2}\mu_{CH4}VT$).

• The ideal adsorbed solution theory agrees well with the observed adsorption capacities and selectivities of CO2/CH4 mixture.

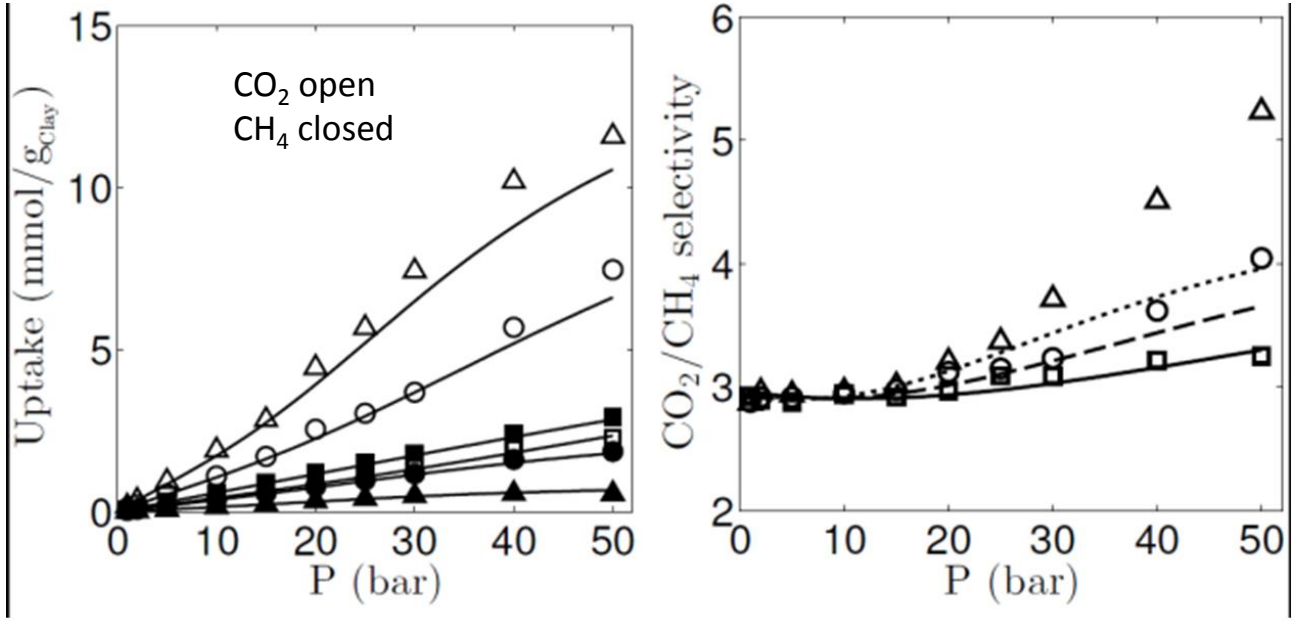

• CO_2 mole fractions: 0.2 (squares), 0.5 (circles), 0.8 (triangles)
• d=30Å
• Water content of 0.2 g/cm^3

Diffusion of CO2, CH4, and their mixture in montmorillonite clay hydrates

• The diffusion of CO2 in the interlayers of Na-montmorillonite, at constant loading of CO2, is not significantly affected by CH4 for the investigated CO2/CH4 mixture compositions.

• The presence of adsorbed CO2 molecules, at constant loading of CH4, very significantly reduces the self-diffusion coefficients of CH4, and relatively larger decreases in those diffusion coefficients are obtained at higher loadings.

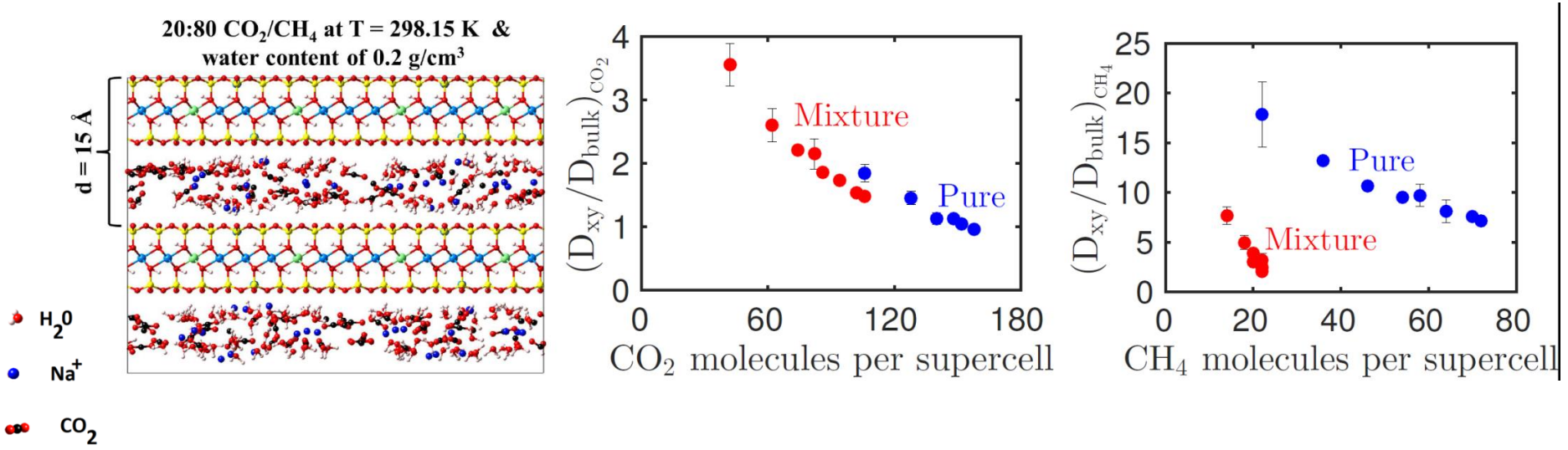

Kadoura et al., 2016b

Adsorption of variably wet scCO2 by montmorillonite (50 °C and 90 bar)

• GCMC simulation study of adsorption of CO2 and water at reservoir conditions ($\mu_{H2O}\mu_{CO2}VT$).

• The intercalation of CO2 in the dehydrated inter-layer is inhibited, followed by the swelling of the interlayer region due to uptake of water and CO2 as the RH increases.

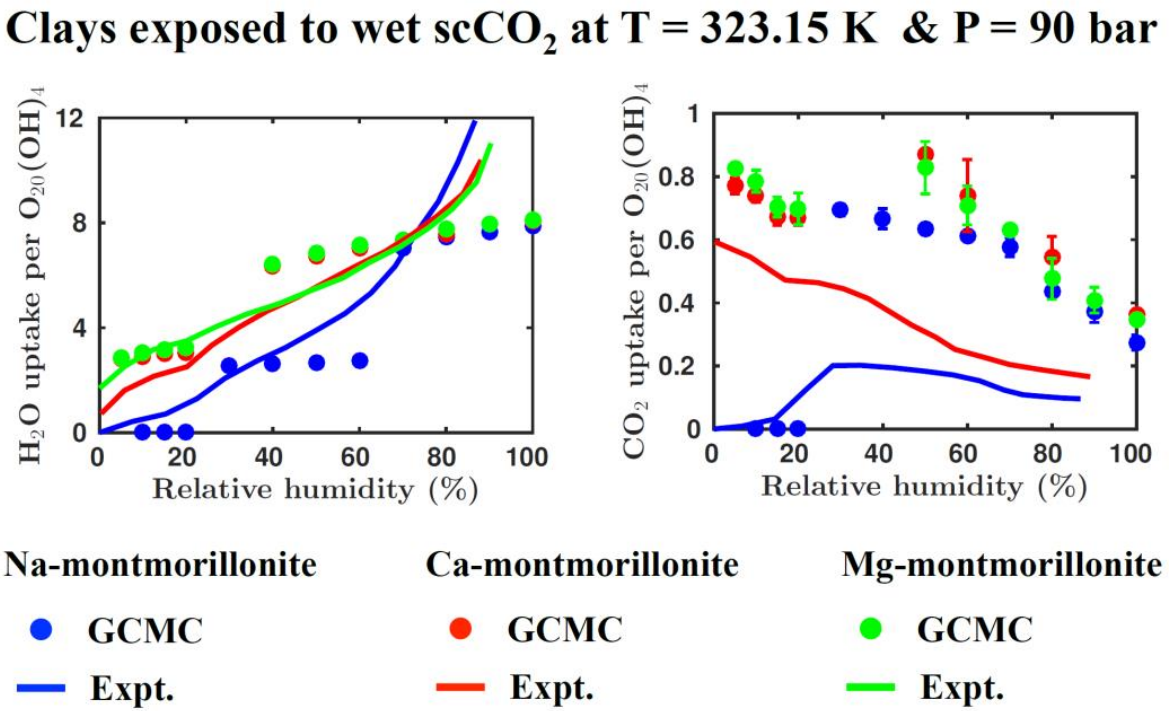

Kadoura et al., 2017

Diffusion of CO2 in montmorillonite clay hydrates at 50 °C and 90 bar

• MD simulation study of CO2 and water at reservoir conditions (NVT).

• The diffusion of CO2 in each hydration state is mostly independent of the type of cation in accordance with the fact that CO2 molecules hardly migrate into the first hydration shell of the interlayer cations.

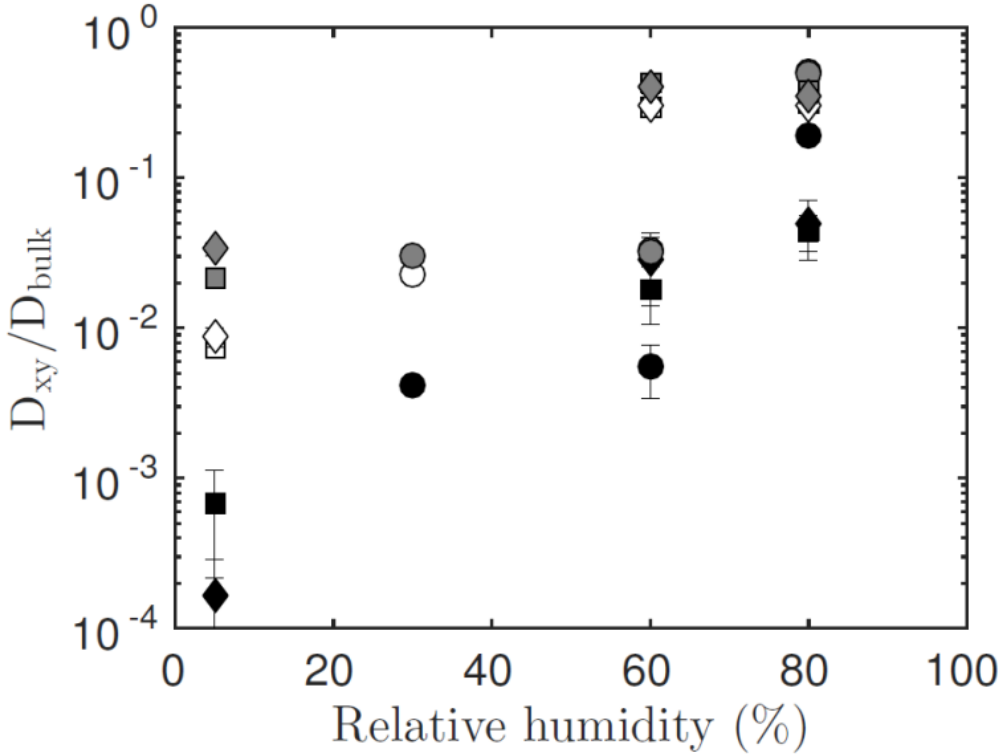

• Na- (circles), Ca- (squares), and Mg-montmorillonite (diamonds)
• ions (black-filled symbols), H2O (open symbols), and CO2 (gray-filled symbols)

Radial distribution function (RDF)

The RDF for species B around A

$$g_{A-B}(r) = \frac{1}{4\pi\rho_B r^2}\frac{dN_{A-B}}{dr}$$

- ρ_B - number density of atoms B
- dN_{A-B} - average number of atom B around a central atom A between the distance of *r* and *r* + *dr*.

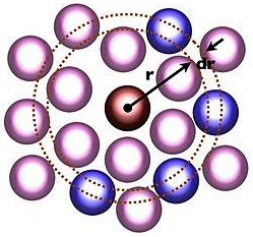

ion-H2O oxygen

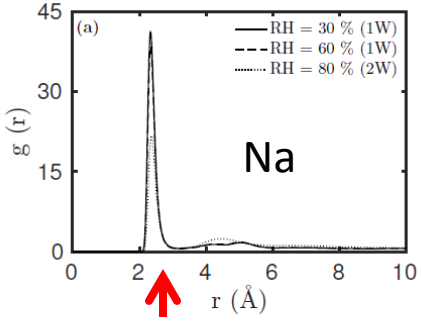

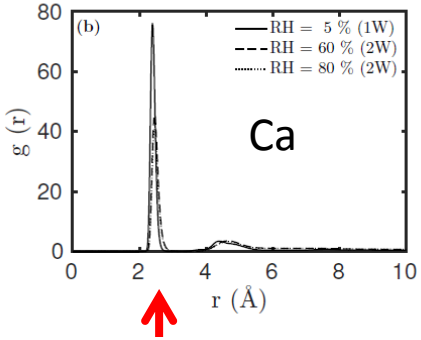

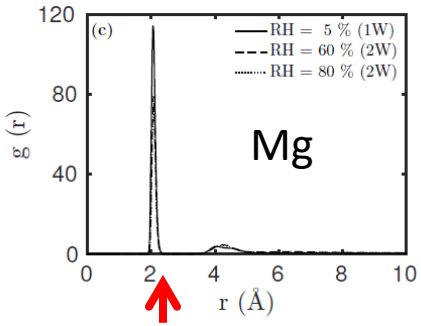

ion-CO2 oxygen

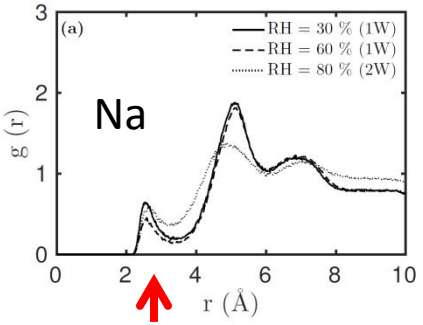

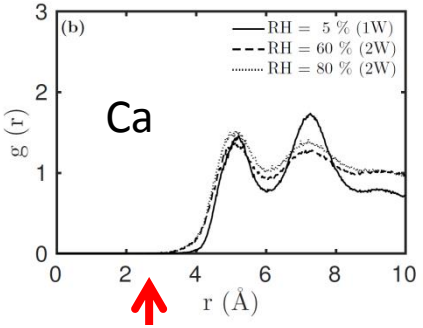

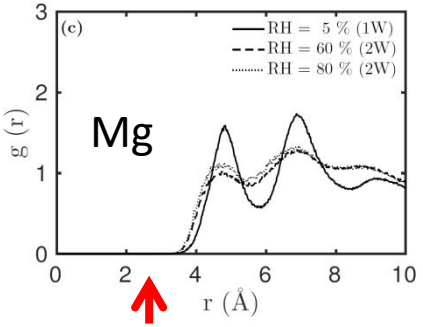

Conclusions

Clay hydrates at 25 °C

• Quantitative agreement of simulated water uptake and self-diffusion coefficients of water and ions in clays with experimental data.

CO2/CH4 mixtures in clay hydrates at 25 °C

• Attributed to their multilayer adsorption, CO2 and methane (to a lesser extent) molecules also favorably adsorb on clay minerals with intermediate water contents.

• The self-diffusion coefficients of methane in the clay interlayers decrease in the presence of CO2. No effect of CH4 on CO2.

scCO2 in clay hydrates at 50 °C and 90 bar

• The diffusion of CO2 in each hydration state is mostly independent of the type of cation in accordance with the fact that CO2 molecules hardly migrate into the first hydration shell of the interlayer cations.